Z. Phys. A 355, 101–105 (1996)

ZEITSCHRIFT
FÜR PHYSIK A
© Springer-Verlag 1996

Reaction rate for two–neutron capture by ^{4}He

V.D. Efros*, W. Balogh, H. Herndl, R. Hofinger, H. Oberhummer

Institute of Nuclear Physics, Technical University Vienna, Wiedner Hauptstrasse 8–10, A-1040 Wien, Austria

Received: 22 December 1995
Communicated by B. Povh

Abstract. Recent investigations suggest that the neutrino–heated hot bubble between the nascent neutron star and the overlying stellar mantle of a type–II supernova may be the site of the r–process. In the preceding α–process building up the elements to $A \approx 100$, the ^{4}He(2n,γ)^{6}He– and ^{6}He(α,n)^{9}Be–reactions bridging the instability gap at $A = 5$ and $A = 8$ could be of relevance. We suggest a mechanism for ^{4}He(2n,γ)^{6}He and calculate the reaction rate within the α+n+n approach. The value obtained is about a factor 1.6 smaller than the one obtained recently in the simpler direct–capture model, but is at least three orders of magnitude enhanced compared to the previously adopted value. Our calculation confirms the result of the direct–capture calculation that under representative conditions in the α–process the reaction path proceeding through ^{6}He is negligible compared to ^{4}He(αn,γ)^{9}Be.

PACS: 25.40.Lw; 25.40.Ny; 97.10.Cv

1 Motivation

Many calculations of the two–step radiative capture reactions of astrophysical interest have been done by now in the framework of the single–particle direct–capture model. An accuracy of the model was not known to a sufficient degree and its assessment by performing a few–body type calculation is of interest. This is accomplished in the present work for the ^{4}He(2n, γ)^{6}He reaction.

In the past years a new neutron–rich astrophysical scenario taking place in the neutrino–heated hot bubble between the nascent neutron star and the overlying stellar mantle of a type–II supernova has been proposed [1]–[5]. The material, originally in nuclear statistical equilibrium (NSE) at high temperature, is expanded and cooled so rapidly that not all the α–particles have time to reassemble. In this environment most nucleons are either in the form of free neutrons or bound in α–particles. The nucleosynthesis in the neutrino bubble takes place in subsequent steps: first, α–particles are formed from the free nucleons. Then, in the following α–process, nuclei up to about $A \approx 100$ are produced [1]. Finally, the neutrino bubble is also an ideal site for the r–process synthesizing the elements of about $A \geq 100$ [1, 6, 7].

The bottleneck of the above nucleosynthesis processes is the formation of nuclei with mass numbers $A \geq 9$ from the nucleons and α–particles, because two–step processes have to be involved in bridging the instability gaps at $A = 5$ and $A = 8$ (see Fig. 1). Due to the lack of neutrons in hydrostatic helium burning in red giants, these instability gaps have to be bridged by the triple–alpha reaction ^{4}He(2α,γ)^{12}C which proceeds as a two–step process $\alpha + \alpha \leftrightarrow {}^8$Be and ^{8}Be($\alpha$,$\gamma$)^{12}C. However, in the α–process where neutrons are available the instability gaps can also be overcome by the reaction ^{4}He(αn,γ)^{9}Be which is much more efficient in the α–process than the triple–alpha reaction rate [1, 5].

Another reaction chain could also be of importance. This chain starts with ^{4}He(2n,γ)^{6}He and is then continued by ^{6}He(α,n)^{9}Be, thereby closing the instability gaps at $A = 5$ and $A = 8$ (see Fig. 1). Here one should take into account that the abundance of free neutrons for the α–process is of the order of 10^{20-30} neutrons cm^{-3} [1, 6] and that the yield of the α2n reaction forming ^{6}He is proportional to $Y_\alpha Y_n^2$ while the yield of the 2αn reaction is proportional to $Y_\alpha^2 Y_n$. (The notation Y_α and Y_n stands for the concentrations of alphas and neutrons, respectively.) The rate of the ^{4}He(2n,γ)^{6}He reaction was estimated in Ref. [8] and found to be very small. However, as it is shown below the main mechanism of the reaction was missed in that study. We thus investigate whether the rate of the reaction is enhanced to a sufficient degree due to this main mechanism under representative conditions. While we are using a three–body model of the process the same issue was studied in a recent independent paper [9] using a simpler direct–capture model.

The ^{4}He(2n,γ)^{6}He–reaction is also of special interest because experimental data of the nucleus ^{6}He show features characteristic for halo nuclei [10, 11]. This is indicated by the special character of the α–spectra for the decay of the $J^\pi = 2^+$ level at $E = 1.8$ MeV in ^{6}He and the measurement of an abnormally large electromagnetic–dissociation cross

* *Permanent address*: Kurchatov Institute, Institute for General and Nuclear Physics, SU–123182 Moscow, Russia

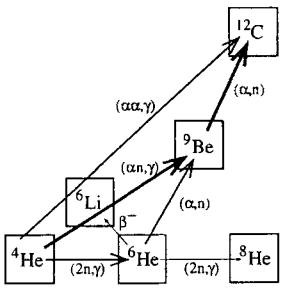

Fig. 1. Possible two–step processes involved in bridging the instability gaps at $A = 5$ and $A = 8$. The main reaction flow under typical conditions in the α–process is indicated by thick arrows, the thinner arrows represent almost negligible reaction flows

section [12, 13]. We note as well that the strength functions for the reverse reaction were calculated in Ref. [14] in the framework of an approach treating all the three final–state particles on equal footing.

2 The model

Let us formulate our model for calculating the ^{4}He(2n,γ)^{6}He reaction rate. We adopt a two–step mechanism for the process. In the first step the p–wave $3/2^-$ resonant state of ^{5}He is formed and the reaction proceeds through a wing of this resonance. Calculations of two–step reactions proceeding through the low–energy wing of a resonance are well known from the triple–alpha process. However, the mechanism of the reaction we are considering proves to be different. In analogy with the triple–alpha process, a transition of a p–wave neutron to the resonant state of ^{6}He followed by a E2 capture to the ground state of ^{6}He would be the second step of the reaction. However there exists an alternative possibility, namely a non–resonant E1–capture of an s–wave neutron. The latter process proves to dominate strongly the reaction in our case. This occurs because of both the lower multipolarity and the absence of a Coulomb or a centrifugal barrier suppressing this transition. We thus adopt this process as the second step of the reaction. The resonant E2–contribution will be commented on below. We use the three–body α+n+n representation of the nuclear system in our calculations.

The reaction rate per particle triplet for ^{4}He(2n,γ)^{6}He, in analogy to the triple–alpha process, is given by [15, 16]

$$\langle 2n^4He\rangle = 2\int_0^\infty dE_1 \frac{\hbar}{\Gamma\left(^5He, E_1\right)} \frac{d\langle n^4He\rangle(E_1)}{dE_1} \times \int_0^\infty dE_2 \frac{d\langle n^5He\rangle(E_1,E_2)}{dE_2}, \quad (1)$$

where E_1 and E_2 are relative energies in the (^{4}He+n)– and (^{5}He+n)–system, respectively. The quantity $\Gamma\left(^5He, E_1\right)$ is an energy–dependent width of ^{5}He, whereas the integrands $d\langle n^4He\rangle(E_1)/dE_1$ and $d\langle n^5He\rangle(E_1,E_2)/dE_2$ are transport cross sections $\sigma(E)v$ [17] for the first and second step, respectively, times the corresponding Maxwell distributions $\sim \sqrt{E}\exp(-E/kT)$.

The first step of the reaction is represented by the first integral in Eq. (1) [15, 16]. An equilibrium between the production and the decay for the population of ^{5}He is assumed here. The relative production rate of ^{5}He is given by $\sigma_1(E_1)v_1$. The total production cross section σ_1 coincides with the elastic (^{4}He+n) cross section as neutron emission of ^{5}He is the only possible exit channel. The relative decay rate is given by $\Gamma\left(^5He, E_1\right)/\hbar$. The integrand is the ratio of the ^{5}He particle density at given E_1 to the product of net α and n particle densities at the equilibrium. To calculate the energy dependent width $\Gamma\left(^5He, E_1\right)$ we need a (^{4}He+n)–potential. It was obtained by scaling the depth and range of the folding potential to the experimental energy and width of the ^{5}He ground state. Both these quantities are exactly reproduced by our potential and $\sigma_1(E_1)$ is also reproduced reasonably well. The values 0.89 MeV [18] and 0.76 MeV were adopted as the Breit–Wigner ^{5}He energy and width, respectively.

The value of the width was deduced [19] from the most recent experiment [20]. In Ref. [20] itself a significantly larger value of the width was reported and we would like to explain the difference between the two values. In Ref. [20] the spectrum of that work was fitted by the expression of the form

$$\frac{\Gamma_R(E_{n\alpha})}{[E_{n\alpha} - E_{res} - \Delta(E_{n\alpha})]^2 + \left[\frac{\Gamma_R(E_{n\alpha})}{2}\right]^2} \quad (2)$$

times a smooth function in the (n $-$ α) relative energy $E_{n\alpha}$. Here $\Gamma_R(E) = 2\gamma^2 P(E)$ and $\Delta(E) = -\gamma^2[S(E) - S(E_{res})]$ where γ^2 is the reduced width, and P and S are the penetrability and the shift function defined as usual. The value of $\Gamma_R(E_{res})$ was then reported as a width. However, this R–matrix value is known to differ from the physical width determining the lifetime of a system. Just the latter width Γ determines the energy-dependent width in Eq. (1) and it can be obtained from the location of the pole $E_{n\alpha} = E_0 - i\Gamma/2$ of the factor (2). This width was found in Ref. [19] and the value obtained is close to the older estimates [18].

To calculate the second step reaction rate $\langle n^5He\rangle$, the ^{5}He(n,γ)^{6}He cross section is required. As explained above, we consider the electric dipole transition E1 from an incident s–wave. The cross section is given by

$$\sigma_2(E_1,E_2) = \frac{2\pi}{81}\left(\frac{E_\gamma}{\hbar c}\right)^3 \frac{e^2}{\hbar v_2} \mid I \mid^2 \quad (3)$$

with

$$I = \frac{1}{k_2}\int_0^\infty dr_1 \int_0^\infty dr_2 u_b(r_1) r_1 u_{sc}(E_2, r_2) \times r_2^2 f_{\ell=1,j=3/2,}(r_1, r_2) \quad , \quad (4)$$

where $E_\gamma = E_1 + E_2 + Q_{12}$ is the energy of the photon, with $Q_{12} = 0.98$ MeV being the Q–value of the reaction ^{4}He(2n,γ)^{6}He. In Eq. (4) the coordinates r_1 and r_2 are the distances between the valence neutron and the α–core or the center of mass of ^{5}He, respectively. The quantities v_2 and k_2 are the relative velocity and wave number in the entrance channel (^{5}He+n) of the second step. The quantity $u_b(r_1)/r_1$ represents the radial part of the quasi–bound wave function of the ^{5}He resonance, and $u_{sc}(E_2, r_2)/r_2$ is the radial part of the (^{5}He+n) scattering wave function. The function $f_{\ell=1,j=3/2}(r_1, r_2)$ is the radial component in the expansion

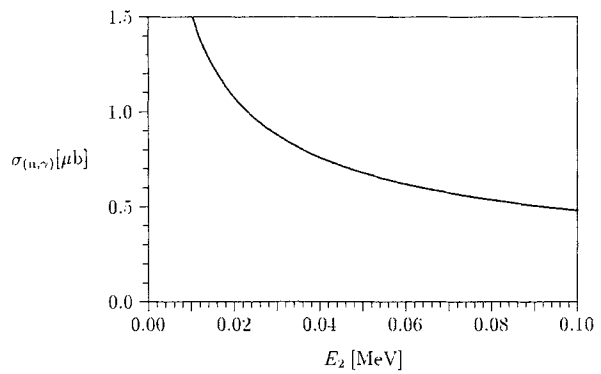

Fig. 2. Calculated cross section for ^{5}He(n,γ)^{6}He

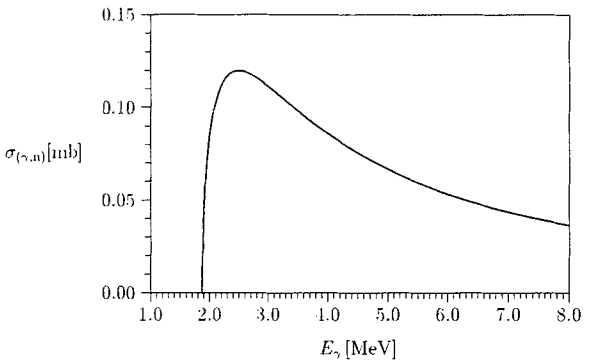

Fig. 3. Calculated cross sections for ^{6}He(γ,n)^{5}He

$$\Psi\left(^6\mathrm{He}\right) = \sum_{j\ell} f_{\ell j}(r_1, r_2)\left[\chi_{\ell j}\left(\hat{\mathbf{r}}_1, \sigma_{1z}\right)\chi_{\ell j}\left(\hat{\mathbf{r}}_2, \sigma_{2z}\right)\right]_{J=0} \quad (5)$$

of the α+n+n ground–state wave function. Here $\chi_{\ell j}$ are angular–momentum functions with orbital momenta ℓ (necessarily equal to each other) and total angular momenta $j = \ell \pm 1/2$, σ_{1z} and σ_{2z} are spin variables of the valence neutrons, and the brackets [...] denote vector coupling. Only the ($\ell = 1, j = 3/2$)–component may contribute to the cross section. The ^{6}He wave function is normalized to unity and the scattering wave function is normalized as $u_{\mathrm{sc}} \rightarrow \sin(kr_2 + \delta)$ in the asymptotic region.

The ground–state wave function $u_{\mathrm{b}}(r_1)$ of ^{5}He was obtained as the Siegert solution to the (^{4}He+n) Schrödinger equation and this solution was taken inside the centrifugal barrier and normalized there to unity (see e.g. [21]). The Siegert solution is an eigenfunction corresponding to the boundary condition for a decaying system and inside the barrier it represents the contribution of a resonance to continuum wave functions. Its absolute value decreases inside the barrier and increases in the outer region. The cut–off radius 7.425 fm was taken at the point of a minimum of $\mid u_{\mathrm{b}} \mid$. Replacement of this complex–energy ($E_0 - i\Gamma/2$) solution by the real–energy E_0 scattering solution with the same cut–off radius leads to less than only 1% difference in the second–step cross section. This shows both that the resonance contribution is a predominant one and that the cut–off radius has been chosen correctly. Variation of this radius, e.g., by ± 1.5 fm changes the cross section by not more than 20%. (Reasonable variations of the cut–off radii give even narrower limits.) The above-mentioned (^{4}He+n) folding potential was used to obtain u_{b}.

To calculate the scattering wave function $u_{\mathrm{sc}}(E_2, r_2)$ we construct the optical (^{5}He+n)–potential by using the folding procedure [22, 23]. We first reproduced the matter density distribution for ^{4}He by means of a simple Gaussian with the r.m.s. matter radius of 1.469 fm deduced from the r.m.s. charge radius of 1.676 fm [24]. To obtain the density distribution for ^{5}He, we folded the ^{4}He–density distribution with the above–mentioned wave function $u_{\mathrm{b}}(E_1, r_1)$. Finally, we used again the folding procedure to obtain the potential. Due to abnormally large separations between the valence neutrons and the α core in the final–state ^{6}He halo nucleus the cross section is largely enhanced. The outer free-motion parts of the u_{b} and u_{sc} functions contribute predominantly to Eq. (4) due to the same reason. If one replaces the (^{4}He+n) potential we used above by the square–well potential whose range and depth are fitted to the position and width of the ^{5}He resonance the reaction rate obtained changes by less than 1% and thus it is insensitive to the form of the potential. An accurate three–body wave function of ^{6}He (see [11]) was used in our calculations. Originally, it was given in LS–coupling and in the form of an expansion over hyperspherical harmonics and we present it in the form of Eq. (5).

While we included the formation of the ^{5}He($3/2^-$) resonance as the first step of the reaction we neglected the contribution from the broad $1/2^-$ resonance. Taking into account Eq. (1) the relative $1/2^-$ contribution may be roughly estimated as

$$[\sigma_{1/2}(E)\Gamma_{3/2}w_{1/2}][\sigma_{3/2}(E)\Gamma_{1/2}w_{3/2}]^{-1} \quad (6)$$

where σ's are elastic cross sections, Γ's are widths and w's are weights of the $f_{\ell=1,j}$ components with $j = 1/2$ and 3/2 in the ^{6}He wave function from Eq. (5). The weights we calculated are $w_{3/2} = 0.87$ and $w_{1/2} = 0.049$. The component entering Eq. (4) thus dominates the ^{6}He wave function. Substituting these values into (6) along with the value of $\Gamma_{1/2} \simeq 4$ MeV [18] we obtain $0.01\sigma_{1/2}(E)/\sigma_{3/2}(E)$. The ratio of the cross sections is less than unity. Thus the contribution of the ^{5}He($1/2^-$) resonance to the reaction rate is negligible.

3 Reaction rates

The calculated cross section for ^{5}He(n,γ)^{6}He can be parametrized by $\sigma = 0.152/\left(E_2\,[\mathrm{MeV}]\right)^{1/2}$ [μb] and it is depicted in Fig. 2. Furthermore, in Fig. 3 the cross section for the inverse process ^{6}He(γ,n) ^{5}He, as obtained from the principle of time–reversal invariance [25, 26], is shown. The cross sections given in these figures were obtained by assuming that ^{5}He exists exactly at the resonance energy $E_1 = 0.89$ MeV. The ^{5}He(n,γ)^{6}He cross section exhibits the $1/v$–behavior corresponding to incident s–waves. The ^{6}He(γ,n)^{5}He cross section shown in Fig. 3 is about three orders of magnitude higher than the maximum value that was originally used for the determination of the reaction rates of ^{4}He(2n,γ)^{6}He and ^{6}He(γ,2n)^{4}He by Fowler et al. [8] (cf. below).

The obtained reaction rate can be parametrized in the following way:

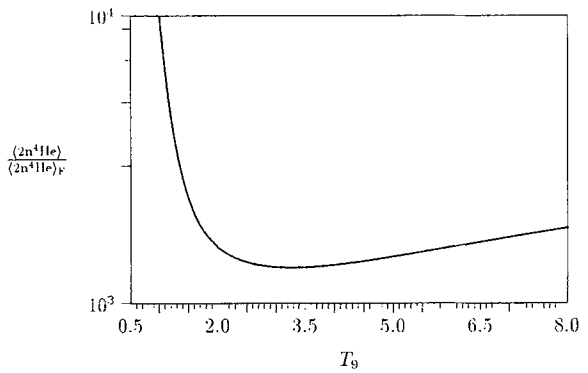

Fig. 4. Ratio of calculated reaction rate of ^{4}He(2n,γ)^{6}He for $T_9 = 0.5 - 8.0$ and the maximum of the previous adopted value [8]

Table 1. Parameters of the reaction rate for ^{4}He(2n,γ)^{6}He calculated in our three–body model

	$0.1 \leq T_9 \leq 2$	$2 < T_9 \leq 15$
a	0.00265	0.293
b	2.55	−0.351
c	0.181	−5.24

$$N_A^2 \langle 2n^4He \rangle = a(T_9)^b \exp\left(\frac{c}{T_9}\right) 10^{-8}\,\mathrm{cm^6\,s^{-1}\,mol^{-2}} \quad , (7)$$

where the parameters a, b, c are listed in Table 1 for the two temperature regions $0.1 \leq T_9 \leq 2$ and $2 < T_9 \leq 15$ (T_9: temperature in units of 10^9 K).

The inverse reaction rate λ_γ per nucleus per second can be calculated by using the RevRatio [8]

$$\lambda_\gamma = \mathrm{RevRatio} \times N_A^2 \langle 2n^4He \rangle \ \mathrm{s^{-1}} \quad . \quad (8)$$

The RevRatio is parametrized in the following way

$$\mathrm{RevRatio} = 1.08(T_9)^3 \exp\left(\frac{-11.3}{T_9}\right) 10^{20}\,\mathrm{cm^{-6}\,mol^2} \quad . \quad (9)$$

As shown in Fig. 4, the reaction rate for ^{4}He(2n,γ)^{6}He calculated with the help of our three–body model is more than three orders of magnitude larger than the maximum of the previously adopted value [8]. This is mainly due to the non–resonant E1–transition of the second step ^{5}He(n,γ)^{6}He, which dominates the cross section, and which was not taken into account in Ref. [8]. We have also obtained an estimate comparable to the results in Fig. 4 using the direct–capture model.

The huge enhancement of the reaction rate obtained can simply be demonstrated as follows. Let us estimate the ratio of the second–step non–resonant transport cross section $\langle \sigma v \rangle_{nr}$ to the resonant one. To simplify the reasoning, let us consider the case of higher temperatures such that kT is comparable to or larger than the width Γ_1 of ^{5}He (T larger than about 10^{10} K). Below it will be convenient to treat the $\langle \sigma v \rangle_{nr}$ value as an average transition probability. This implies that the ^{5}He+n relative wave function is normalized to $\exp(i\mathbf{kr})$ plus the scattered wave at large distances. The resonant second–step transition disregarded in our calculations proceeds through the first excited state ^{6}He(2^+) lying within the width of the broader ^{5}He resonance. The quantity $\langle \sigma v \rangle$ for this transition can be estimated as (c.f. [17])

Table 2. Comparison of the reaction rates of the photodisintegration ^{6}He(γ,2n)^{4}He (second column) and ^{6}He(α,n)^{9}Be (third column) for different temperatures (first column)

T_9	λ_γ	$N_A\langle {}^6\mathrm{He}\alpha\rangle$
0.5	1.28×10^{-2}	6.45×10^5
0.8	7.71×10^{2}	3.16×10^6
1.0	4.36×10^{4}	6.69×10^6
1.5	1.66×10^{7}	2.64×10^7
2.0	4.87×10^{8}	6.86×10^7
2.5	4.54×10^{9}	1.37×10^8
3.0	2.27×10^{10}	2.26×10^8
5.0	8.50×10^{11}	6.05×10^8

$(\hbar^2/2\mu)\mu^{-1/2}\Delta^{-3/2}x^{3/2}\exp(-x)\hbar w_r$ where Δ is the position of the ^{6}He resonance with respect to the (^{5}He+n) threshold, $x = \Delta/kT$, μ is the reduced mass for (^{5}He+n) and w_r is the transition probability pertaining to the transition from the ^{6}He(2^+) quasi–bound state to the ground state. The quantity Δ equals to $(E_r - E_1)$ where E_r is the absolute position of the ^{6}He(2^+) resonance and E_1 is the energy of ^{5}He. This quantity should be averaged over the distribution of E_1 giving $\bar{\Delta}(T) \simeq \Gamma_1$. The ratio $\langle \sigma v \rangle_{nr}/w_r$ of the two transition probabilities equals to the squared ratio of absolute values of electromagnetic transition matrix elements. The transitions considered are E1 and E2, respectively, and this ratio can thus be estimated as $R^3[(2l+1)/k_\gamma R]^2$ where $l = 2$, $k_\gamma \simeq 10^{-2}\,\mathrm{fm^{-1}}$ is the photon momentum, $R \simeq 4.5$ fm [11] is the average distance between a (^{4}He+n) subsystem and the other outer neutron in the ^{6}He nucleus and the R^3 factor comes from the difference in normalizations of the initial state wave functions entering the transition matrix elements. As a result we arrive at the rough estimate

$$25\left[\frac{(\hbar k_\gamma)^2}{2\mu}\right]^{-1}\left(\frac{\hbar^2}{\mu R^2}\right)^{-1/2}\Gamma_1^{3/2}\bar{x}^{-3/2}\exp(\bar{x}) \simeq 5 \cdot 10^3 \bar{x}^{-3/2}\exp(\bar{x})$$

for the ratio of the reaction rates, where $\bar{x} \simeq \Gamma_1/kT$.

The rate obtained in our three-body calculation is about a factor of 1.6 smaller than the simpler single–particle direct–capture rate given in Ref. [9]. Therefore, we reach the same conclusion as in Ref. [9], i.e. for the trajectories relevant to the r–process given in Ref. [4] (the last 16 trajectories given in Table III) the reaction rate of the ^{4}He(2n,γ)^{6}He obtained is stronger by a factor of three than the triple–α reaction, but is still weaker by approximately two orders of magnitude than the ^{4}He(αn,γ)^{9}Be reaction.

With respect to the photodisintegration of ^{6}He our calculations show that for the same trajectories as given above, the beta decay of ^{6}He and ^{6}He(2n,γ)^{8}He are slower by about 10 and 11 orders of magnitude, respectively (the reaction rate for ^{6}He(2n,γ)^{8}He is given in [27]). The reaction ^{6}He(α,γ)^{10}Be is smaller by about two orders of magnitude. The only reaction which can compete with the photodisintegration is the reaction ^{6}He(α,n)^{9}Be. The cross section for the inverse reaction ^{9}Be(n,α)^{6}He was measured by Stelson and Campbell [28] in the energy range from 0.7 to 4.4 MeV. From this the reaction rate of ^{6}He(α,n)^{9}Be was deduced. A comparison of the rate with the photodisintegration rate is given in Table 2 for different temperatures. While the rate for the photodisintegration is multiplied with the density ρ in

units $g\,cm^{-3}$ and the ^{6}He abundance in the network, the rate for the α capture is multiplied with the square of the density and the abundances of ^{6}He and α. Therefore, under representative conditions (cf., Ref. [1]) with $\rho = 5 \times 10^4\,g\,cm^{-3}$ and $Y_\alpha = 0.225$ most of the produced ^{6}He can be processed further on to ^{9}Be. Even at $T_9 = 5.0$ alpha capture by ^{6}He is still more important than photodisintegration. However, it has to be noted that under representative conditions in the α–process the reaction path proceeding through ^{6}He is still negligible compared to the reaction ^{4}He(αn,γ)^{9}Be.

In conclusion, we have considered a new mechanism of the two–neutron capture by the ^{4}He nucleus which leads to a more than three order of magnitude enhancement with respect to the value adopted by Fowler et al. [8]. We have performed a simplified three–body calculation of the reaction rate that proved to be in accordance with the prediction of the simple direct–capture model within a factor of two. The inverse reaction of the photodisintegration of ^{6}He has also been studied. Our cross–section for the photodisintegration via formation of the intermediate ^{5}He state can be verified in experiments on ^{6}He break–up on heavy targets at low energies, of the type performed last years [29, 30] for the ^{11}Li nucleus. The results obtained have a relevance to other 2N radiative capture processes as well.

The authors are indebted to I.J. Thompson for help in their work and to J.S. Vaagen and M.V. Zhukov for valuable discussions on halo nuclei. Useful discussions with J. Görres, M. Wiescher and M.J. Balbes are acknowledged. This work was supported by the Fonds zur Förderung der wissenschaftlichen Forschung in Österreich (project P10361–PHY), by the Österreichische Nationalbank (project 5054) and by the International Science Foundation and Russian Government (grant J4M100).

References

1. Woosley, S.E., Hofmann, R.D.: Astrophys. J. **395**, 202 (1992)
2. B.S. Meyer, B.S., Howard, W.M., Mathews, G.J., Woosley, S.E., Hoffmann, R.D.: Astrophys. J. **399**, 656 (1992)
3. Howard, W.M., Gloriely, S., Rayet, M., Arnould, M.: Astrophys. J. **417**, 713 (1993)
4. Woosely, S.E., Wilson, J.R., Mathews, G.J., Hofmann, R.D., Meyer, B.S.: Astrophys. J. **433**, 229 (1994)
5. Witti, J., Janka, H.-Th., Takahashi, K.: Astron. and Astrophys. **286**, 841 (1994)
6. Kratz, K.L., Bitouzet, J.-P., Thielemann, F.-K., Möller, P., Pfeiffer, B.: Astrophys. J. **403**, 216 (1993)
7. Takahashi, K., Witti, J., Janka, H.-Th.: Astron. and Astrophys. **286**, 857 (1994)
8. Fowler, W.A., Caughlan, G.R., Zimmerman, B.: Ann. Rev. Astron. Astrophys. **13**, 69 (1975)
9. Görres, J., Herndl, H., Thompson, I.J., Wiescher, M.: Phys. Rev. C **52**, 2231 (1995) and private communication
10. Sakuta, S.B., Ogloblin, A.A., Osadchy, O.Ya., Glukhov, Yu.A., Ershov, S.N., Gareev, F.A., Vaagen, J.S.: Europhys. Lett. **22**, 511 (1993)
11. Zhukov, M.V., Danilin, B.V., Fedorov, D.V., Bang, J.M., Thompson, I.J., Vaagen, J.S.: Physics Rep. **231**, 151 (1993)
12. Balamuth, D.P., Griffioen, K.A., Bush, J.E., Pohl, K.R., Handzy, D.O., Aguirre, A., Sherrill, B.M., Winfield, J.S., Morrissey, D.J., Thoennessen, M.: Phys. Rev. Lett. **72**, 2355 (1994)
13. Tanihata, I.: Nucl. Phys. A **522**, 275c (1991)
14. Danilin, B.V., Zhukov, M.V., Vaagen, J.S., Bang, J.M.: Phys. Lett. B **302**, 129 (1993)
15. Nomoto, K., Thielemann, F.-K., Hiyaji, S.: Astron. and Astrophys. **149**, 239 (1985)
16. Görres, J., Wiescher, M., Thielemann, F.-K.: Phys. Rev. C **51**, 392 (1995)
17. Rolfs, C., Rodney, W.S.: Cauldrons in the Cosmos. Chicago, University of Chicago Press, 1988
18. Ajzenberg–Selove, F.: Nucl. Phys. A **490**, 1 (1988)
19. Efros V.D., Oberhummer, H.: submitted to Phys. Rev. C, 1995.
20. Balbes, M.J., Kramer, L.H., Weller, H.R., Tilley, D.R.: Phys. Rev. C **43**, 343 (1991)
21. Baz, A.I., Zeldovich, Ya.B., Perelomov, A.M.: Scattering, Reactions and Decay in Non–Relativistic Quantum Mechanics. Nauka, Moscow, 1971
22. Kobos, A.M., Brown, B.A., Lindsay, R., Satchler, G.R.: Nucl. Phys. A **425**, 205 (1984)
23. Oberhummer, H., Staudt, G.: in Oberhummer, H., ed.:Nuclei in the Cosmos. Heidelberg, Springer Verlag, 1991 29–59.
24. De Vries, H., De Jager, C.W., De Vries, C.: Atom. Data and Nucl. Data Tabl. **36**, 495 (1987)
25. Blatt, J.M., Weisskopf, V.F.: Theoretical Nuclear Physics (New York, Wiley, 1962)
26. Frauenfelder, H., Henley, E.M.: Subatomic Physics. Englewood Cliffs, Prentice–Hall, 1974
27. Oberhummer, H., Balogh, W., Efros, V.D., Herndl, H., Hofinger, R.: Few–Body Systems Suppl. **8**, 317 (1995).
28. Stelson, P.H., Campbell, E.C.: Phys. Rev. **106**, 1252 (1957)
29. Anne, R. et al.: Phys. Lett. B **250**, 19 (1990)
30. Shimoura, S. et al.: Phys. Lett. B **348**, 29 (1995)